Exploiting $h \to W^*W^*$ Decays at the Upgraded Fermilab Tevatron

Ren-Jie Zhang
Department of Physics, University of Wisconsin, Madison, WI 53706

We study the observability of a Standard Model-like Higgs boson at an upgraded Fermilab Tevatron via the mode $h \to W^*W^*$. We perform detector level simulations for the $gg \to h \to W^*W^* \to \ell\bar{\nu}\bar{\ell}\nu$ and $q\bar{q}' \to W^\pm h \to W^\pm W^* W^* \to \ell^\pm\nu\ell^\pm\nu jj$ channels. We find that with a c. m. energy of 2 TeV and an integrated luminosity of 30 fb^{-1} the signal should be observable at a 3σ level or better for the mass range of 145 GeV $\lesssim m_h \lesssim$ 180 GeV. For 95% CL exclusion, the mass reach is 135 GeV $\lesssim m_h \lesssim$ 190 GeV. We conclude that the upgraded Fermilab Tevatron will have the potential to significantly advance our knowledge of Higgs boson physics.

I. INTRODUCTION

The Higgs boson is an important ingredient of the Standard Model and the chief quarry at present and future collider programs. Based on theoretical arguments, the mass of the Higgs boson is subject to the following generic bounds [1]: (a) The triviality bound, which indicates that the Higgs boson mass (m_h) should be less than about 800 GeV for the SM to be a consistent low-energy effective theory. (b) Vacuum stability bound, which suggests a correlation between the m_h lower bound and the new physics scale Λ beyond which the SM is no longer valid.

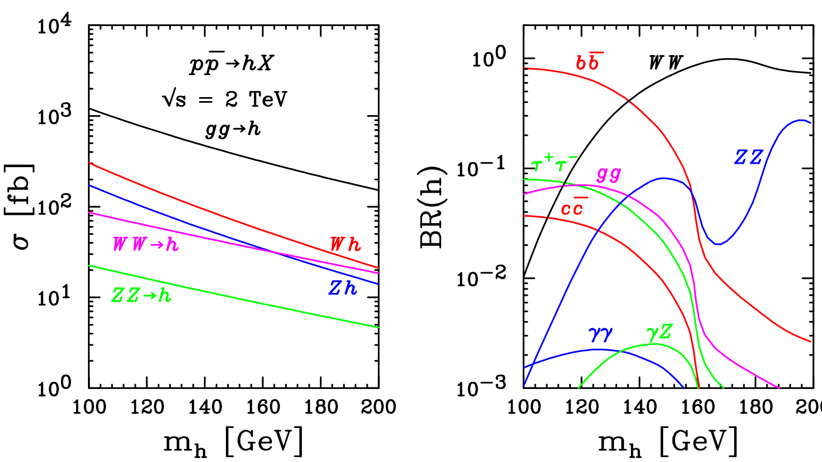

FIG. 1. The leading Higgs boson production cross sections (in fb) versus m_h at the 2 TeV Tevatron. The solid curves are for $gg \to h$, $q\bar{q}' \to W^\pm h$ and $q\bar{q} \to Zh$. The dashed curves are for W^+W^- and ZZ fusion to h. The scale on the right-hand side indicates the number of events per 30 fb^{-1} integrated luminosity. QCD corrections have been included.

On the experimental side [2], the non-observation of Higgs signal at the LEP2 experiments has established a lower bound on the SM Higgs boson mass of 89.8 GeV at a 95% CL. Future searches at LEP2 will eventually be able to discover a SM Higgs boson with a mass up to 105 GeV. The CERN Large Hadron Collider (LHC) is believed to be able to cover up to the full m_h range of theoretical interest, about 1000 GeV.

It has been discussed intensively how much the Fermilab Tevatron upgrade can do for the Higgs boson search. It appears that the most promising processes continuously going beyond the LEP2 reach would be the associated production of an electroweak gauge boson and the Higgs boson, $p\bar{p} \to WhX,\ ZhX$. The leptonic decays of W, Z provide a good trigger and $h \to b\bar{b}$ may be reconstructible with adequate b-tagging. It is now generally believed that for an upgraded Tevatron with a c. m. energy $\sqrt{s} = 2$ TeV and an integrated luminosity $\mathcal{O}(10-30)$ fb^{-1} a SM-like Higgs boson can be observed at a $3-5\sigma$ level up to a mass of about 120 GeV [2]. The Higgs discovery through these channels crucially depends up on the b-tagging efficiency and the $b\bar{b}$ mass resolution. It is also limited by the event rate for $m_h > 120$ GeV. In this talk I shall show that one can greatly extend the Higgs boson reach at the upgraded

Tevatron by exploiting other modes:

- Dilepton+$\not{E}_T$: $gg \to h \to W^*W^* \to \ell\bar{\nu}\bar{\ell}\nu$,
- Like-sign lepton+jets: $q\bar{q}' \to W^{\pm}h \to W^{\pm}W^*W^* \to \ell^{\pm}\nu\ell^{\pm}\nu jj$.

The large production cross-section $gg \to h$ and/or the decay branching ratio $h \to W^*W^*$ for $m_h \geq 135$ GeV make the above modes clear choices for Higgs boson search beyond 135 GeV at the upgraded Tevatron.

To illustrate this point, we show the Higgs boson production cross sections at a 2 TeV upgraded Tevatron and its subsequent decay braching ratio in Fig. 1(a) and 1(b) respectively. We see that the gluon fusion process has the largest total cross section, typically a factor of 4 greater than that of associated productions. The Higgs boson has the increasingly large branching ratio to WW, when $m_h \gtrsim 135$ GeV, the WW decay channel dominates. We have also shown the vector boson fusion process cross sections in Fig. 1(a).

Our signal and background Monte Carlo simulation was performed using the PYTHIA package interfaced with the SHW detector simulation [3]. The production cross-sections for the principal background processes were normalized to $\sigma(WW) = 10.4$ pb, $\sigma(t\bar{t}) = 6.5$ pb, $\sigma(WZ) = 3.1$ pb, and $\sigma(ZZ) = 1.4$ pb.

II. DI-LEPTONS PLUS MISSING TRANSVERSE ENERGY SIGNAL

For the pure leptonic channel, we identify the final state signal as two isolated opposite-sign charged leptons and large missing transverse energy. The leading SM background processes are

$$\begin{aligned} &p\bar{p} \to W^+W^- \to \ell\bar{\nu}\bar{\ell}\nu, \quad ZZ(\gamma^*) \to \nu\bar{\nu}\ell\bar{\ell}, \quad WZ(\gamma^*) \to \ell\bar{\nu}\ell\bar{\ell}, \\ &p\bar{p} \to t\bar{t} \to \ell\bar{\nu}\bar{\ell}\nu b\bar{b}, \quad p\bar{p} \to Z(\gamma^*) \to \tau^+\tau^- \to \ell\bar{\nu}\bar{\ell}\nu\nu_\tau\bar{\nu}_\tau. \end{aligned} \tag{1}$$

We impose the following acceptance cuts:

- Two and only two opposite sign leptons. $p_T(e) > 10$ GeV, $|\eta_e| < 1.5$; $p_T(\mu_1) > 10$ GeV, $p_T(\mu_2) > 5$ GeV, $|\eta_\mu| < 1.5$; $m(\ell\ell) > 10$ GeV, $\Delta R(\ell j) > 0.4$, $\not{E}_T > 10$ GeV.
- Jet veto: (jet$\equiv p_T > 15$ GeV, $|\eta| < 3$.)
  - veto if $p_T^{j_1} > 95$ GeV, or $p_T^{j_2} > 50$ GeV, or $p_T^{j_3} > 15$ GeV,
  - veto if either of the two hard jets (j_1, j_2) has a b-tagging, (assuming b-tagging efficiency $\epsilon_b = 1.1 \times 57\% \tanh(\eta_b/36.05)$.)
- Dilepton opening angles $\phi(\ell\ell) < 160^\circ$, $\theta(\ell\ell) < 160^\circ$.
- $p_T(\ell\ell) > 20$ GeV, $\cos\theta_{\ell\ell\text{-}\not{E}_T} < 0.5$, $M_T(\ell\not{E}_T) > 20$ GeV, where $M_T^2(\ell\not{E}_T) = 2p_T(\ell)\not{E}_T(1-\cos\theta_{\ell\text{-}\not{E}_T})$.
- $m(\ell\ell) < 78$ GeV for $e^+e^-, \mu^+\mu^-$, $m(\ell\ell) < 110$ GeV for $e\mu$.
- Helicity angle of ℓ_1 in the lepton pair rest-frame $-0.3 < \cos\theta^*_{\ell_1} < 0.8$.

One can improve the signal observability further by constructing a likelihood based on some characteristic kinematical variables. The detail can be found in Ref. [5].

In identifying the signal events, it is crucial to reconstruct the mass peak of m_h. Unfortunately, the W^*W^* mass from the h decay cannot be accurately reconstructed due to the two undetectable neutrinos. However, both the transverse mass M_T and the cluster transverse mass M_C, defined as [4]

$$M_T = 2\sqrt{p_T^2(\ell\ell) + m^2(\ell\ell)}, \quad M_C = \sqrt{p_T^2(\ell\ell) + m^2(\ell\ell)} + \not{E}_T, \tag{2}$$

yield a broad peak near m_h and have a long tail below. The cluster transverse mass M_C has a Jacobian structure with a well defined edge at m_h. For a given m_h to be studied, one can perform additional cut optimization. In Table I, we list m_h-dependent criteria for the signal region defined as

$$m_h - 60 < M_C < m_h + 5 \text{ GeV}. \tag{3}$$

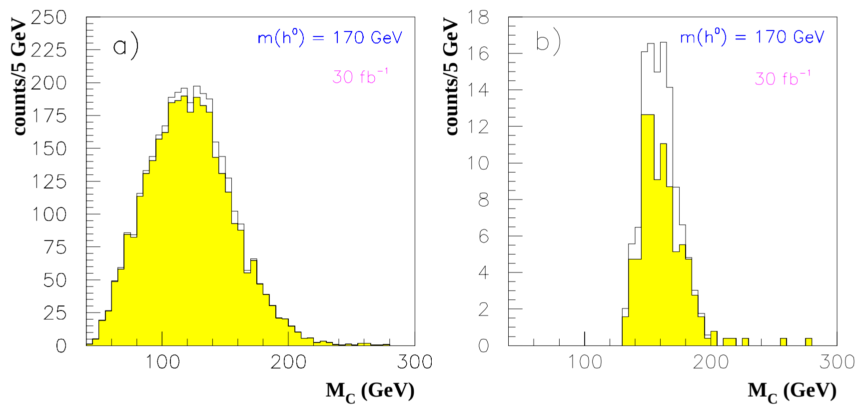

FIG. 2. The leading Higgs boson production cross sections (in fb) versus m_h at the 2 TeV Tevatron. The solid curves are for $gg \to h$, $q\bar{q}' \to W^{\pm}h$ and $q\bar{q} \to Zh$. The dashed curves are for W^+W^- and ZZ fusion to h. The scale on the right-hand side indicates the number of events per 30 fb^{-1} integrated luminosity.

m_h [GeV]	140	150	160	170	180	190
$\cos\theta^*_{\ell_1}$	-	<0.6	0.35	0.35	0.55	0.75
$\not{E}_T$	>25	25	30	35	40	40
$\min[M_T(\ell_1\not{E}_T), M_T(\ell_2\not{E}_T)]$	>40	40	75	80	85	75
$M_T(\ell_1\not{E}_T)$	>60	60	-	-	-	-
$m(\ell\ell)$	<65	65	65	75	85	-
$p_T(\ell\ell)$	>40	50	65	70	70	70
$\theta(\ell\ell)$	<100	100	70	70	90	90
M_T	-	>110	120	130	140	140

TABLE I. Summary of the optimized cuts for various Higgs boson mass.

m_h [GeV]	140	150	160	170	180	190
$gg \to h$ [fb]	2.2	2.4	1.3	0.93	0.85	0.73
associated VH [fb]	0.26	0.31	0.13	0.09	0.06	0.06
VV fusion [fb]	0.12	0.12	0.09	0.06	0.05	0.05
signal sum [fb]	2.6	2.8	1.5	1.1	0.96	0.83
SM bckgrnds [fb]	39	27	4.1	2.3	3.8	7.0
fake $j \to e$ [fb]	5.1	3.4	0.34	0.15	0.08	0.45
bckgrnds sum [fb]	44	30	4.4	2.4	3.8	7.5
S/B [%]	5.8	9.4	34	45	25	11
$S/\sqrt{B}$ [30 fb^{-1}]	2.1	2.8	3.9	3.8	2.7	1.7

TABLE II. Summary table for $h \to W^*W^* \to \ell\bar{\nu}\bar{\ell}\nu$ signal for m_h = 140−190 GeV and various SM backgrounds after the kinematical and likelihood cuts. W+fake refers to the background where a jet mimics an electron with a probability of $P(j \to e) = 10^{-4}$. The backgrounds are independent of m_h.

We illustrate the effect of the optimized cuts of Table I in Fig. 2, where the cluster tranverse mass distribution for a $m_h = 170$ GeV signal and the summed backgrounds, normalized to 30 fb^{-1}, are shown before (a) and after the final cuts (b). A clear excess of events from the Higgs signal can be seen in Fig. 2(b). It is important to note that before application of the final cuts, the dominant backgrounds are WW and the W+fake with other sources accounting for less than 10% of the total. Moreover, for 30 fb^{-1} integrated luminosity, the statistical error in the background is less than 2% before application of the final cuts. We therefore argue that one should be able to normalize the SM background curve (WW) with sufficient precision to unambiguously identify a significant excess attributable to Higgs boson signal.

Our final results for the channel $h \to W^*W^* \to \ell\bar{\nu}\bar{\ell}\nu$ are summarized in Table II. We have included the contributions to $h \to W^*W^*$ from the vector boson fusion channels as well as from $W \to \tau\nu \to \ell\nu_\ell\nu$. It can be seen that one may achieve a S/B of at least 6% for 140 GeV$< m_h <$ 190 GeV and reach 45% for $m_h = 170$ GeV. The statistical significance, $S/\sqrt{B}$, for 30 fb^{-1} integrated luminosity, is 3σ or better for $150 < m_h < 180$ GeV.

III. LIKE-SIGN DI-LEPTON PLUS JETS SIGNAL

The contributing channels to this mode are $Wh \to WW^*W^* \to \ell^\pm\nu\ell^\pm\nu jj, Wh \to WZ^*Z^* \to \ell^\pm\nu\ell^\pm\ell^\mp jj, Zh \to ZW^*W^* \to \ell^\pm\ell^\mp\ell^\pm\nu jj, Zh \to ZZ^*Z^* \to \ell^\pm\ell^\mp\ell^\pm\ell^\mp jj$. We identify the final state signal as two isolated like-sign charged leptons plus jets. A soft third lepton may be present. The SM backgrounds are

$$p\bar{p} \to WWW,\ WWZ,\ WZZ,\ ZZZ,\ t\bar{t}W,\ t\bar{t}Z \to \ell^\pm\ell^\pm jj\ X, \tag{4}$$

$$p\bar{p} \to W^\pm Z(\gamma^*) + jj \to \ell^\pm\ell^\pm jjX,\quad ZZ(\gamma^*) + jj \to \ell^\pm\ell^\pm jjX,\quad t\bar{t} \to \ell\bar{\nu}jjb\bar{b}, \tag{5}$$

$$p\bar{p} \to Wjj,\ Z(\gamma^*)jj + \text{fake}.$$

Although the triple gauge boson production in Eq. (4) constitutes the irreducible backgrounds, the $WZjj$, $t\bar{t}$ through b or c semileptonic decay and the background from $j \to e$ fakes turn out to be larger.

We impose the following cuts

- Two same-sign leading leptons. $p_T(\ell) > 10$ GeV, $|\eta_\ell| < 1.5$, $m(\ell\ell) > 10$ GeV, $0.3 < \Delta R(\ell j) < 6$, $\not{E}_T > 10$ GeV (For a muon, further demand that the scalar sum of additional track momenta within 30° be less than 60% of the muon momentum.)
- Jets criteria: (jet$\equiv p_T > 15$ GeV, $|\eta| < 3$.)
  - $2 \le N_{jet} \le 3$
  - Leading jet $|\eta_{j_1}| < 1.5$, $2 < N_{charged\ track} < 12$. Sub-leading jet $|\eta_{j_2}| < 2.0$.
  - Veto if $p_T^{j_3} > 30$ GeV, or any of the jets has a b-tagging.
- $m(jj) < 110$ GeV, $\Sigma_j|p_T^j| < 150$ GeV.
- $\cos\theta^*_{\ell_1} < 0.95$.

m_h [GeV]	120	130	140	150	160	170	180	190	200
signal sum [fb]	0.093	0.20	0.34	0.52	0.45	0.38	0.29	0.20	0.16
bckgrnd channels	WZ	ZZ	WW	$t\bar{t}$	VVV	$t\bar{t}V$	$W/Z\ jj$+fake	Sum	
σ [fb]	0.27	0.06	0.01	0.15	0.07	0.02	0.26	0.83	
S/B [%]	11	24	41	63	54	46	35	24	19
$S/\sqrt{B}$ [30 fb^{-1}]	0.56	1.2	2.0	3.1	2.7	2.3	1.7	1.3	0.96

TABLE III. $Vh \to \ell^\pm\ell^\pm jj$ signal for $m_h = 120-200$ GeV and the SM backgrounds after the kinematical cuts.

With these cuts, we present the results for the signal and backgrounds in Table III. We can see that for a given m_h, the S/B is larger than that for the di-lepton plus $\not{E}_T$ signature, reaching as high as 63%. One can consider further optimization of cuts with m_h dependence. However, the rather small signal rate for a 30 fb^{-1} luminosity limits the statistical significance. Also, the systematic uncertainty in the background may be worse than the pure leptonic channel.

IV. DISCUSSIONS AND CONCLUSION

We combine our results from the two channels in Fig. 3. Based on statistical effects only, we conclude that with a c. m. energy of 2 TeV and an integrated luminosity of 30 fb^{-1} the Higgs boson signal via $h \to W^*W^*$ should be observable at a 3σ level or better for the mass range of 145 GeV$\lesssim m_h \lesssim$ 180 GeV. For 95% CL exclusion, the mass reach is 135 GeV$\lesssim m_h \lesssim$ 190 GeV. These limits degraded a little bit if a 10% systematic error is assumed, as shown in Fig. 3(b). (Systematic errors are estimated by simultaneously scaling the background upward and the expected signal downward by 10%.)

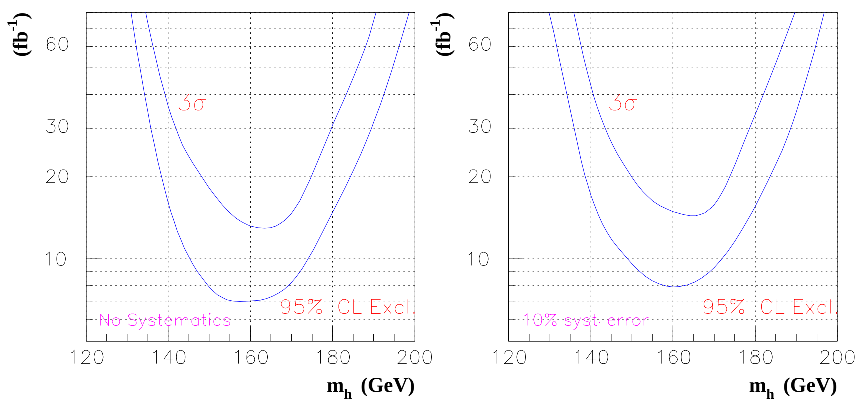

FIG. 3. The leading Higgs boson production cross sections (in fb) versus m_h at the 2 TeV Tevatron. The solid curves are for $gg \to h$, $q\bar{q}' \to W^\pm h$ and $q\bar{q} \to Zh$. The dashed curves are for W^+W^- and ZZ fusion to h. The scale on the right-hand side indicates the number of events per 30 fb^{-1} integrated luminosity.

To conclude, I have demonstrated that the $h \to W^*W^*$ channel has excellent potential to extend the Higgs boson reach at the upgraded Tevatron.

Acknowledgments: It is a pleasure to thank T. Han and A. Turcot for collaboration. This work was supported in part by a DOE grant No. DE-FG02-95ER40896 and in part by the Wisconsin Alumni Research Foundation.

[1] H. Haber, summary talk for the Higgs Working Group, http://fnth37.fnal.gov/funnelweb/hab/; M. Carena, summary talk for the Higgs Working Group, http://fnth37.fnal.gov/funnelweb/carena_summary/.
[2] W. M. Yao, these proceedings; J. Hobbs, these proceedings, and references therein.
[3] SHW2.0, by J. Conway, available at http://www.physics.rutgers.edu/jconway/soft/shw/shw.html.
[4] T. Han and R.-J. Zhang, Phys. Rev. Lett. **82**, 25 (1999).
[5] T. Han, A.S. Turcot and R.-J. Zhang, Phys. Rev. **D59**, 093001 (1999).